Supplementary Information

Title: Probing the picosecond kinetics of photosystem II cores *in vivo*.

Lijin Tian[a], Shazia Farooq[a], and Herbert van Amerongen*[a,b].

[a] Laboratory of Biophysics, Wageningen University, PO Box 8128, 6700 ET, Wageningen, The Netherlands

[b] MicroSpectroscopy Centre, Wageningen University, PO Box 8128, 6700 ET, Wageningen, The Netherlands

Comparison between the streak-camera data and the TCSPC data of the PAL mutant with fully open RCs of PSII *in vivo*
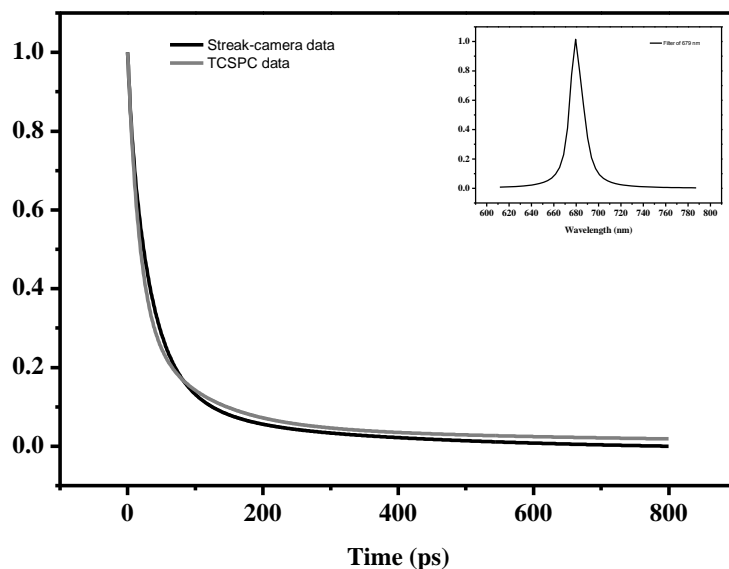

Figure s1: The streak camera data and the TCSPC data. To compare the decay curves fairly, both datasets were reconstructed based on the fitting results without including the IRFs. At the same time, the streak-camera data was calibrated by multiplying the DAS with the transmission spectrum (indicated as inset) of the 679 nm interference filter that was used in the TCSPC measurements, thus making sure that only the emitted photons within that wavelength interval were counted. Measuring conditions: a) TCSPC, laser power-17 µW, λ_{exc} = 440 nm, with 679 nm interference filter added in front of the detector; b) Streak camera, laser power-10 µw, λ_{exc} = 400 nm. Note that in the TCSPC measurement, the excitation spot is ~100 times bigger than in the streak-camera experiments, which ensures that the intensity is low enough to keep the RCs fully open.

In general, the results obtained with the two setups are very similar to each other, although the TCSPC decay is slightly faster in the beginning. Both kinetics are also slower than the kinetics observed for PSII cores isolated from *Synechococcus elongatus* (see the main manuscript of this work).

Target analysis:

To complete a fair comparison between the time-resolved fluorescence decay of PSII with open RCs in our paper and in previously published articles, we have fitted our results to the same model schemes as proposed by van der Weij et al. in 2011[1] and Miloslavina et al. in 2006[2], respectively. Interestingly, all the models listed below can provide equally good fits of the data.

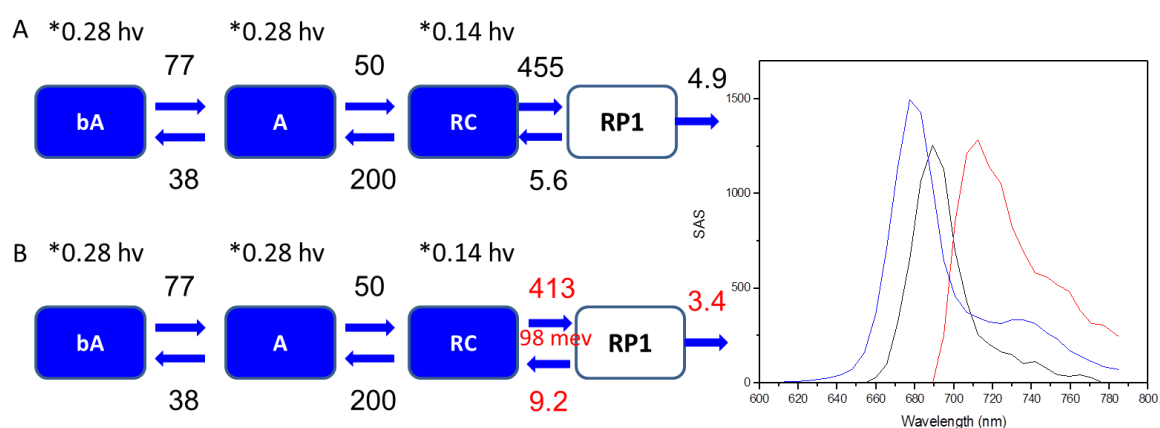1) Model I by van der Weij et al. in 2011

Figure s2: Model with slow EET from CP43/47 to RC. The model A represents the compartmental model used by van der Weij et al. in 2011 together with the EET/CS rates. The model B is used on the data set obtained in this work, with several EET transfer rates fixed (in black) while the charge-transfer rates and charge recombination rates were left free (in red). The obtained SAS are shown on the right.

As shown in Figure s2, the primary charge separation rate of 413 ns^{-1} is almost identical to the reported value of 455 ns^{-1} by Van der Weij et al., but the charge recombination rate is faster, while the second charge separation rate is slower. The calculated ΔG is -98 meV which is smaller than the on reported by Van der Weij et al. in 2011, namely, -110 meV.
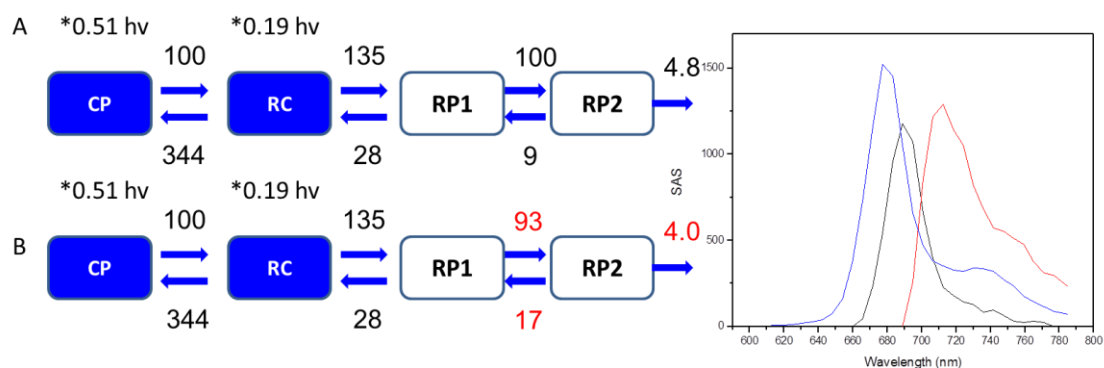
2) Model II by van der Weij et al. in 2011

Figure s3: Models with fast equilibration between core antenna and RC. Model A) is reported in ref C.D. van der Weij et al. in 2011. Model B) shows the fitting results of the dataset in this work.

As the fitting results in Figure s3 show, the free fitting values in model B) are very close to their corresponding ones in model A), the main change concerns the charge recombination rate from RP2 to RP1, which is almost doubled in B).

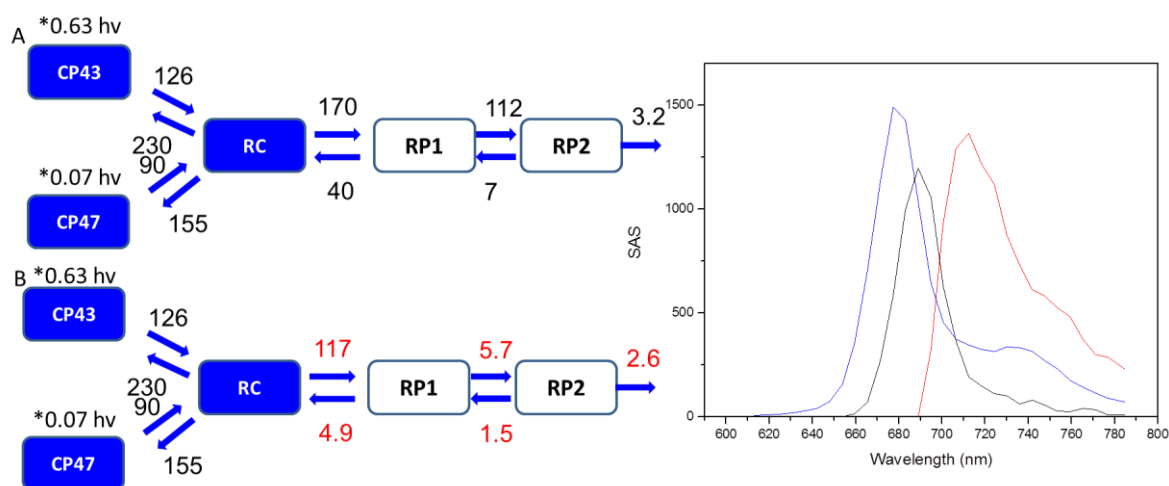3) Model proposed by Miloslavina et al. in 2006

Figure s4: Model with fast equilibration between core antenna and RC with CP43 and CP47 separated in the model (their spectra were forced to be same).

With this model (Figure.s4), it seems that the second RP is not needed when the RC is open *in vivo*, since the rate of charge recombination is far slower than the primary charge separation rate.

Sample_400 nm_exc.	PSI				PSII			PSI/PSII ratio (PSI-96 pigments;PSII-35 pigments)
	PSI_bulk	PSI_red						
BE_298K	1.0	0.06			N.A.			N.A.
PAL_298K_open	1.0	0.06			Ant*RC*		RP1	0.55
					0.7		0.0	
PAL_298K_closed	1.0	0.06			Ant*RC*	RP1	RP2	0.55
					0.7	0.0	0.0	
BE_77K	1.0	712 nm	715 nm	726 nm	N.A.			N.A.
		0.02	0.02	0.02				
PAL_77K_Model I	1.0	0.02	0.02	0.02	Ant*RC*	RP1	690 nm	0.55
					0.7	0.0	0.0	
PAL_77K_Model II	1.0	0.02	0.02	0.02	Ant*RC*	RP1	690 nm	0.55
					0.7	0.0	0.0	

Table s1: Input values for target analysis of BE and PAL mutants, and the calculated PSI/PSII ratios.

Based on these initial energy inputs in PSI and in PSII, we can roughly estimate the PSI/PSII RC ratio in the PAL mutant. In view of the number of Chls ~96 per PSI core vs ~35 per PSII core[3,4], a RC ratio of PSI/PSII of ~0.55± 0.10 was calculated. The error bar of ± 0.10 is estimated based on different repeated measurements and tested models.

Constraints that are used in the target analysis in the main text:

Constraints in general

1) Energy input on each pool is fixed in the fitting, values are listed in Table S1;
2) Spectral shape constraints---a skewed Gaussian shape was used for all the SAS spectra[5];
3) Zero constraint—Amplitudes of the SAS for the radical pair pools (RP) were forced to be zero at all wavelengths (Figure 3, Figure 6&7 in the main text).

Specific constraints for target analysis 1 (at room temperature)—Figure 3:

4) Red SAS of open RC as shown in Figure 3 was forced to be zero up to 670 nm;
5) Rate constants for PSI were fixed to their corresponding values in the PSI model as described before in ref 6&7[6,7].

Specific constraints for target analysis 2 (model I at 77K)—Figure 6:

6) In the model for the BE mutant, energy transfer rates from pigments_690 nm to pigments_715 nm and to pigments_712 nm were forced to be same, which enables us to provide a mathematical description of the PSI kinetics at 77K；
7) Parameters of PSI in the PAL mutant were fixed based on the model of the BE mutant at 77K ;
8) Three pools of 680 nm (cyan) in the PSII branch in PAL mutant were forced to have the same spectra.

Specific constraints for target analysis 3 (model II at 77K)—Figure 7:

9) Same as 6);
10) Same as 7);
11) Two pools of 680 nm (cyan) in the PSII branch in PAL mutant were forced to have the same spectra.

Reference:

(1)   van der Weij-de Wit, C. D.; Dekker, J. P.; van Grondelle, R.; van Stokkum, I. H. M. *J Phys Chem A* **2011**, *115*, 3947-3956.

(2)   Miloslavina, Y.; Szczepaniak, M.; Muller, M. G.; Sander, J.; Nowaczyk, M.; Rogner, M.; Holzwarth, A. R. *Biochemistry-Us* **2006**, *45*, 2436-2442.

(3)   Jordan, P.; Fromme, P.; Witt, H. T.; Klukas, O.; Saenger, W.; Krauss, N. *Nature* **2001**, *411*, 909-917.

(4)   Umena, Y.; Kawakami, K.; Shen, J. R.; Kamiya, N. *Nature* **2011**, *473*, 55-60.

(5)   I.H.M. van Stokkum, DS Larsen, R van Grondelle. Biochimica et Biophysica Acta (BBA)-Bioenergetics,2004, 1657 (2), 82-104.

(6)   V. Chukhutsina, L. Tian. G Ajlani, H van Amerongen, in *Photosynthesis Research for Food, Fuel and Future*, eds. T. Kuang, C. Lu and L. Zhang, Zhejiang University Press, Hangzhou, Beijing, 2010, pp. 465-467.

(7)   L. Tian, I. H. M. van Stokkum, R. B. M. Koehorst, A. Jongerius, D. Kirilovsky and H. van Amerongen, *J.Am. Chem. Soc.*, 2011, **133**, 18304-18311.